J. Fluid Mech. (1981), *vol.* 105, *pp.* 219–238
Printed in Great Britain

Effect of a sharp edge on an excited jet

By N. W. M. KO†
Engineering Department, University of Cambridge

(Received 11 May 1979 and in revised form 30 September 1979)

An experimental study of an excited jet interrupted normally by a 90° sharp edge is described in this paper. Based on schlieren technique, it is possible to distinguish three flow regions: the main jet flow, the wake flow behind the sharp edge and the redirected flow on the surface. By following the individual articially excited jet vortices, it is possible to observe the structure and to estimate the convection velocity of these vortices in the three flow regions. By comparison with the results of the uninterrupted jet, the effect of the sharp edge is obtained and presented.

1. Introduction

Recent studies on the suppression of the jet noise of aircraft engines, for example, of Arctander, Hodge & Tate (1975) and Frasca (1975) were concerned with the effect of the mixer nozzle, ejector and ejector/suppressor on the jet noise produced. Although reduction of jet noise was achieved, airplane performance penalties have precluded their application.

The existence of large-scale or coherent structure in the mixing region of jet has been observed by investigating either the unexcited or excited jet (see, for example, Crow & Champagne 1971; Lau, Fisher & Fuchs 1972; Chan 1974; Moore 1977; Fuchs & Michel 1977). The evidence of the dominating coherent structure suggested another approach for the suppression of jet noise. Attempts at breaking up this coherent structure with the intention of suppressing the jet noise have been made by Scharton & White (1972), Arndt, Tran & Barefoot (1974) and Arndt, Fuchs & Michel (1978). Various model suppressors were inserted near or downstream of the nozzle exit; however, the devices tested were found ineffective. Further, the above investigations concerned mainly the noise reduction in the far field without considering the effect of the suppressor on the coherent structure itself.

Even though the structure of the unexcited and excited jet flow has been well studied, the disruption by an outside body such as a flat surface normal to the jet and the effect on the jet itself have not been studied. Although the study on the free-jet impingement has been made by Donaldson & Snedeker (1971) and Donaldson, Snedeker & Margolis (1971), it mainly concerned the flow characteristics of the fully developed jet impinging directly on a fairly large surface. The impingement of the jet on part of the surface has not been included in the investigation of the above-mentioned workers.

Vortex-shedding from thin flat plates and isolated aerofoils parallel to the free stream has been investigated by, to mention only a few, Bauer (1961), Tam (1974) and Davis (1975). Effort was mainly concentrated on the regular vortex wake generated by

† On long leave from Department of Mechanical Engineering, University of Hong Kong.

the flat plates and the aerofoils. For flow normal to the plate or surface vortex shedding from the leading edge of a delta wing at small angle has also been visualized (Batchelor 1967, plate 22). Further, the work of Sforza *et al.* (1978) concerned the flow field of the leading-edge vortices behind slender delta wings. The study concentrated on the mean velocity contours and their direction behind different slender delta wings. Nevertheless, data of the fluctuating components and the characteristics of the leading edge vortices were not included.

Thus, the present study is part of a detailed investigation which was aimed at obtaining a better understanding on the behaviour of the coherent structure when it was interrupted or disturbed by an outside body. In this paper the simple case of an interrupted flat surface – a 90° sharp edge placed normally to the jet flow – is presented. By using schlieren technique it was possible to study the complicated flow field of the interrupted jet, the wake behind the sharp edge and the redirected flow on the surface. In a future paper the more complicated case of the 180° flat surface will be presented. Coupled with pressure measurements it was hoped that the behaviour of the interrupted or disturbed coherent structure could be better understood and the change in the noise characteristics could be better known.

2. Apparatus

The model jet rig used for the present investigation has been described by Heavens (1978, 1980). The nozzle was a cone of semi-angle 15° with an inlet diameter of 75 mm and an exit diameter D of 12·5 mm. Air was supplied by an eccentric vane compressor and no attempt was made to absorb the inherent noise before the nozzle exit.

The jet was excited by an acoustic pulse which was generated by a spark discharge of energy 5 J. The spark gap was positioned on the axis of a plenum chamber of diameter 0·2 m and length 0·35 m and was about 22 exit diameters upstream of the nozzle exit. The gap was situated at the focus of a parabolical reflector of diameter 100 mm, resulting in a weak direct wave and a strong N-wave due to reflexion. The N-wave has a duration of 50 μs and a rise time of 15 μs. The spark discharged a single pulse which needed about 700 μs to arrive at the nozzle exit. The detailed development of the individual vortices in the jet flows was followed by successive schlieren photographs having a time delay interval of 38 μs. It was found that this interval was sufficient to observe the detailed development and to obtain the characteristics of the individual vortices reasonably well.

The 90° sharp edge used had a thickness of 6·4 mm. On the two edges there was a flat portion of 1 mm before tapering off at an angle of 45° (see figures 2–5). All through the present study the sharp edge was held broadside-on and normally to the jet and the tapered part on the downstream side. The vertex and the line of symmetry of the sharp jet were always pointing towards the central axis of the jet and the two edges were always extended far into the entrainment region. Furthermore, the location of the sharp edge was limited to the region within the first three diameters downstream of the nozzle exit and $y/D > 0$. The projected area of the sharp edge over the nozzle was about 2–12 per cent of the nozzle exit area. The exit Mach number was 0·5.

The jet was visualized with a Z-type schlieren system with mirrors of diameter 100 mm. A horizontal knife-edge (perpendicular to the jet axis) was used for all the schlieren photographs. The illumination was by means of an argon jet light-source of a spark duration of 0·2 μs. It was triggered by an acoustic spark with an adjustable time delay. At any time delay two sets of schlieren photographs were made such that averages of the flow structures could be obtained.

3. Excited jet

An abbreviated sequence of schlieren photographs of the excited jet is shown in figure 1. As have been shown by similar results at other Mach numbers of Heavens (1980), the introduced weak wave and the strong N-wave generate the corresponding vortex rings (figure 1 *a*). They are very similar to the vortex rings of large cross-section of Moore (1977) when the jet was acoustically excited under full drive level. The 'weak vortex' or the vortex ring generated by the weak wave tends to be more diffuse than the vortices of the N-waves. During its propagation downstream this weak vortex maintains its size right up to its disappearance, starting at an axial distance of about 1·8 D from the nozzle exit (table 1).

Although the 'first N-vortex' or the vortex ring of the first peak of the N-wave is fairly intense during its initial state of generation (figure 1 *a*), it experiences fairly rapid deterioration during its propagation downstream (figure 1 *b*, *c*). This vortex also disappears at an axial distance of about 1·8 D downstream from the nozzle exit (table 1). During its propagation downstream the size of the vortex is to a great extent maintained.

The 'second N-vortex' or the vortex ring generated by the second intense peak of the N-wave becomes the dominant one even within half a diameter downstream (figure 1 *b*). It grows in size as it propagates downstream. At an axial distance of 1·8 D the vortex diameter is approximately 1·5 times that at the nozzle exit (figure 1 *e*, *a*). This vortex becomes more diffuse as it propagates further downstream and seems to lose its distinct ring-like structure at about 2·5 D (figure 1 *f*). It more or less disappears at about 3·3 D (table 1).

The convection velocities of the three vortices were obtained from the x–t diagram of their propagation downstream (Roshko 1976; Moore 1977; Heavens 1980). The gradients, and hence the convection velocities, were estimated from the data by linear regression. In the present investigation the correlation coefficient (r^2) of the linear regression usually has value higher than 0·99. The estimated convection velocities $(\overline{U}_c)_j$ of the three vortices are produced in table 2. This means that the weak and first N-vortex are convecting at the same velocity, 0·6 $\overline{U}_0$, while the stronger second N-vortex is slower, 0·4 $\overline{U}_0$. This slower propagation of the stronger second N-vortex may be due to the increase in the size of the vortex (Batchelor 1967, p. 523). For the other two vortices the lack of growth may be responsible for the higher convection velocity.

The convection velocities shown in table 2 agrees well with the transport velocity of a planar jet of Rockwell & Niccolls (1972) and of the wave group velocity from schlieren photographs of Moore (1977). For the planar jet of high Reynolds number, 10800, the transport velocity was 0·5 $\overline{U}_0$ to 0·6 $\overline{U}_0$, the actual value depending on the axial distance from the nozzle exit (Rockwell & Niccolls 1972). This transport velocity agrees very well with the convection velocities of the weak and first N-vortex of 0·6 $\overline{U}_0$. Further, the results obtained by Moore (1977), 0·5 $\overline{U}_0$ and 0·7 $\overline{U}_0$, which were also dependent on the axial distance, agree well with those of the present investigation.

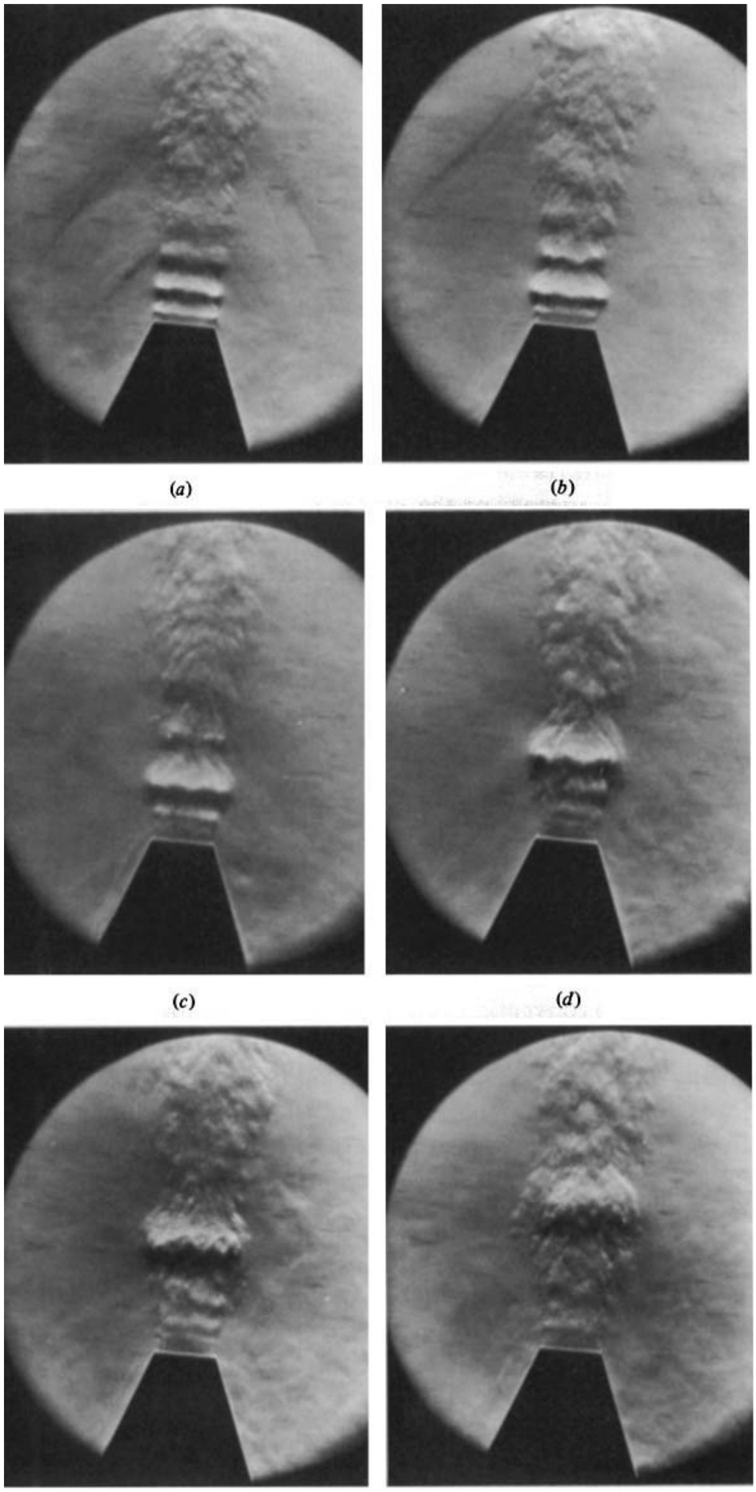

(a) (b) (c) (d) (e) (f)

FIGURE 1. Schlieren photographs of the excited jet (without sharp edge). First frame time delay = 725 μs. Time between successive frames = 75 μs.

Location of sharp edge		Weak	First	Second
x/D	y/D	vortex	N-vortex	N-vortex
—	—	1·8 D	1·8 D	3·3 D
0·3	0·15	1·4 D	1·4 D	2·1 D
0·55	0·15	1·3 D	1·4 D	2·2 D
0·75	0·15	1·7 D	1·8 D	2·7 D
1·0	0·15	1·7 D	1·7 D	2·7 D?
1·5	0·15	1·8 D	1·8 D	2·7 D?
2·0	0·15	1·7 D	1·9 D	2·7 D?
0·3	0·35	1·4 D	1·4 D	2·3 D
0·55	0·35	1·4 D	1·4 D	2·4 D
0·75	0·35	1·6 D	1·7 D	2·7 D
1·0	0·35	1·7 D	1·9 D	2·9 D?
1·5	0·35	1·7 D	1·9 D	2·7 D?

TABLE 1. Approximate axial position at which the vortices in the main jet flow disappear.

Location of sharp edge		$(\bar{U}_c)_i/\bar{U}_0$		
		Weak	First	Second
x/D	y/D	vortex	N-vortex	N-vortex
—	—	0·6	0·6	0·4
0·3	0·15	0·4	0·6	0·4
0·55	0·15	0·5	0·5	0·4
0·75	0·15	0·5	0·5	0·4
1·0	0·15	0·5	0·5	0·4
1·5	0·15	0·5	0·6	0·4
2·0	0·15	0·5	0·5	0·4
3·0	0·15	0·6	0·5	0·4
0·3	0·35	0·5	0·5	0·4
0·55	0·35	0·5	0·6	0·4
0·75	0·35	0·5	0·6	0·4
1·0	0·35	0·5	0·6	0·4
1·5	0·35	0·5	0·6	0·4
3·0	0·40	0·5	0·6	0·4

TABLE 2. Convection velocity of the vortices in the main jet flow.

4. Excited jet with sharp edge

4.1. *Main jet flow*

The presence of the sharp edge induces a more complicated flow pattern of the jet. Besides the main jet flow, a wake is formed behind the sharp edge and a flow is set up under its surface. This section will deal mainly with the main jet flow and the effect of the sharp edge on the three vortices generated. An abbreviated sequence of schlieren photographs with the sharp edge at $x/D = 0{\cdot}3$, $y/D = 0{\cdot}15$ was obtained and is shown in figure 2. From the photographs the weak vortex is found to be fairly diffuse and starts to disappear fairly early. The first and second N-vortex, however, are still distinct.

Directly downstream from the sharp edge no vortex structure associated with either the weak or the first N-vortex is found (figure 2a). For the second N-vortex

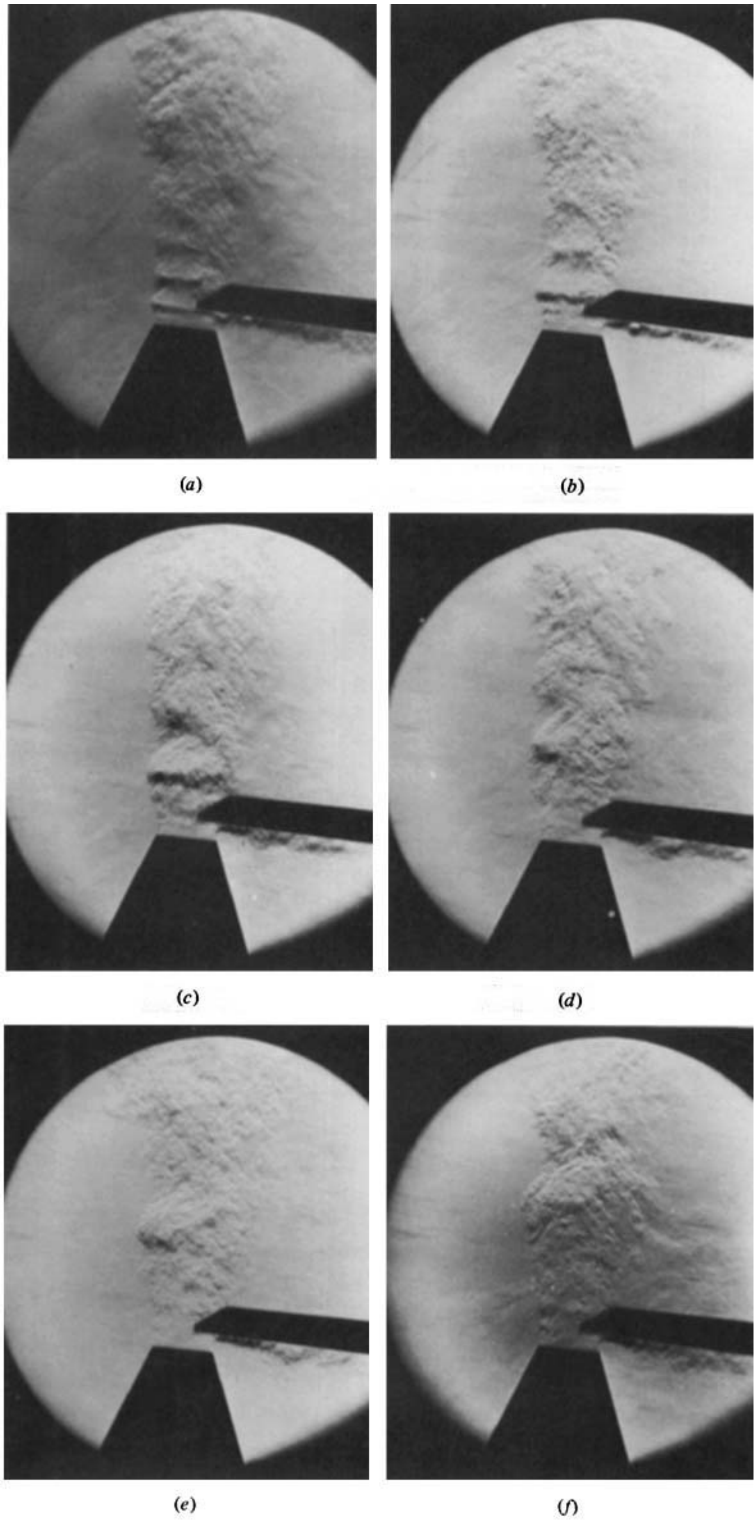

FIGURE 2. Schlieren photographs of the excited jet (with sharp edge). Location of sharp edge: $x/D = 0{\cdot}3$, $y/D = 0{\cdot}15$. Other details as for figure 1.

the vortex is found extending partly into the wake of the sharp edge (figure 2*b*, *c*). This extended part of the vortex is not as distinct as that in the main jet flow and diffuses completely at an axial distance of 1 to $1\frac{1}{2}$ diameters downstream from the nozzle exit (figure 2*d*). Furthermore, this diffused area is expended as it propagates downstream. This means that the distant or coherent part of the second N-vortex reduces in size very rapidly and becomes only a small portion of its former self after a certain distance downstream (figure 2*d*, *e*).

The presence of the sharp edge so close to the nozzle exit also affects the angle of spread of the jet (figure 2*b*). This angle is found to be bigger not only for the boundary immediately downstream from the sharp edge but also for the boundary away from it. Nevertheless, although the angle of spread of the boundary behind the sharp edge is increased, the wavy pattern between the first and second N-vortex is absent (figure 2*c*, *f*) and is mainly due to the dominance of the wake. This means that the uninterrupted or coherent part of the vortex does not extend right to the edge of the wake flow.

Comparison of the vortices shown in figure 2 with those not affected by a sharp edge (figure 1) is interesting. The presence of the sharp edge at such an early stage of the development of the vortices seems to inhibit their proper development. The weak vortex found downstream from the sharp edge is much more diffuse and weaker than when it is not interrupted by the sharp edge. In addition, the weak vortex disappears earlier, at an axial distance of about $1{\cdot}4\,D$ (figure 2*a*). This inhibited development is also observed in the first N-vortex, which seems to disappear at the same axial distance of about $1{\cdot}4\,D$ (figure 2*b*). For the second N-vortex an inhibited development is also found and is responsible for the earlier diffusion and disappearance of this vortex. Near complete disappearance of the remaining part of the vortex is illustrated by figure 2 (*e*) at about $2{\cdot}1\,D$. This distance, as also tabulated in table 1, is much less than that of the uninterrupted jet.

The blockage due to the sharp edge prevents part of the vortex from propagating downstream with the main jet flow. Even though the initial fluid impulse for the vortex may be the same, the total kinetic energy is reduced (Batchelor 1967, p. 523). In view of the disruption of the coherence of the ring structure of the vortex, especially during its initial developing stage, it is not surprising to observe the weaker and earlier diffuse vortices.

The above reasoning is supported by the observed absence of the vortex structure of the weak and first N-vortex directly behind the sharp edge. Because of their lack of strength, they do not maintain their ring-like structure. However, the unblocked part of the stronger second N-vortex maintains its ring-like structure, resulting in the observable, though diffuse, vortex structure directly behind the sharp edge. This attempt to maintain its ring structure may be the cause for the earlier disappearance of the second N-vortex, by about $1{\cdot}2\,D$. For the other two vortices the corresponding distance is only $0{\cdot}4\,D$.

The effect of a smaller blockage of the sharp edge on the vortices can be seen from the schlieren photographs obtained with the sharp edge situated at $x/D = 0{\cdot}3$, $y/D = 0{\cdot}35$ (figure 3). The sharp edge was maintained at the same axial position of $x/D = 0{\cdot}3$ as that in figure 2 but was moved further towards the outer jet boundary. This smaller blockage results in the disruption of the ring vortex being less, so that the vortex structure of the first N-vortex, though slightly more diffuse, is found in the wake directly behind the sharp edge (figure 3*a*). For the second N-vortex the vortex

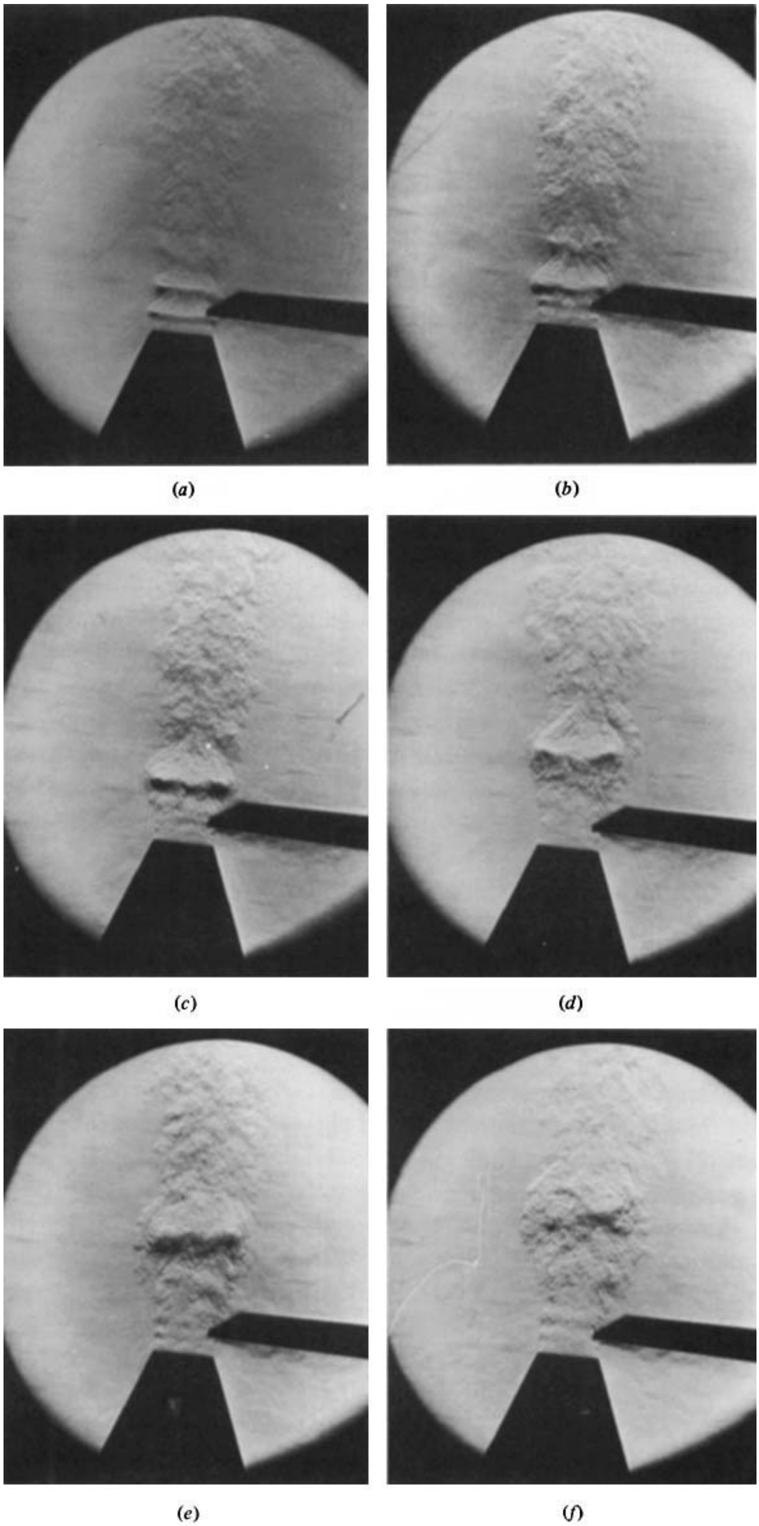

FIGURE 3. Schlieren photographs of the excited jet (with sharp edge). Location of sharp edge: $x/D = 0\cdot3$, $y/D = 0\cdot35$. Other details as for figure 1.

structure is not only immediately behind the sharp edge (figure 3*b*, *c*) but much further downstream (figure 3*e*).

Although the vortex structure is found directly behind the sharp edge at this position of $x/D = 0{\cdot}3$, $y/D = 0{\cdot}35$, the intensity of the vortex itself seems to be about the same as that at $x/D = 0{\cdot}3$, $y/D = 0{\cdot}15$. Furthermore, the three vortices disappear at approximately the same axial position as those with the bigger blockage (table 1).

The schlieren photographs obtained with the sharp edge located at $x/D = 0{\cdot}55$ were also obtained but are not shown in the present paper. The photographs indicate basically the same phenomenon of the vortices as that described above. The approximate axial positions at which the three vortices disappear are roughly the same as those at $x/D = 0{\cdot}3$ (table 1).

A different effect starts to be observed when the sharp edge is positioned further downstream. The schlieren photographs obtained with the sharp edge at $x/D = 0{\cdot}75$, $y/D = 0{\cdot}15$ illustrate stronger vortices than those with the sharp edge placed closer to the nozzle exit (figure 4). This is coupled with the longer life span of all the three vortices (table 1). In addition, the approximate axial position at which the weak vortex and the first N-vortex disappear is about $1{\cdot}7\,D$ which is roughly the same as those of the vortices which are not disturbed by the sharp edge (table 1). For the second N-vortex, however, the approximate position is about $2{\cdot}7\,D$ which is closer to the nozzle exit than that of the undisturbed vortex.

Wavy pattern on the outer boundary away from the sharp edge appears in figure 4(*c*)–(*e*) and in figure 2(*c*)–(*e*). The presence and absence of the wavy pattern may be due to the state of the energy and development of the vortex before its arrival at the sharp edge. For the case of $x/D = 0{\cdot}75$ the more-developed state of the vortex may allow it to continue to develop downstream with sufficient energy, resulting in more entrainment of the ambient air. It may also be due to the more vigorous interaction between the more-developed vortex and the outer boundary of the jet. It is possible that the less-developed state of the vortex in the case of $x/D = 0{\cdot}3$ does not provide sufficient energy for the interaction. For the case of $x/D = 1{\cdot}0$ the lack of development downstream may be the reason for the absence of the wavy pattern. However, further work is required to understand the exact mechanism involved.

This more complete development of the vortex before its interruption is also indicated by the approximate axial position at which the vortex disappears (table 1). At this location of the sharp edge, $x/D = 1{\cdot}0$, $y/D = 0{\cdot}15$, the approximate positions of the three vortices correspond to those of the uninterrupted jet. Schlieren photographs of the excited jet with the sharp edge located further downstream, $x/D > 1{\cdot}0$, have also been obtained but are not shown here. The vortices seem to develop normally, as in the case without interruption by a sharp edge, before their arrival at the edge. The corresponding axial positions at which the vortices disappear agree with those without a sharp edge (table 1). Similarly, when the sharp edge is placed further away from the jet axis, such as at $y/D = 0{\cdot}35$, not much effect on the vortices can be observed from the schlieren photographs. Furthermore, at these positions of the sharp edge, $x/D \geq 0{\cdot}75$, $y/D = 0{\cdot}35$, the axial positions at which the vortices disappear are roughly the same as those of the uninterrupted jet.

The convection velocities of the three jet vortices, when the sharp edge is located at different positions, have also been estimated (table 2). As in the case of the jet without interruption by a sharp edge, the convection velocity $(\overline{U}_c)_j$ was found from the data

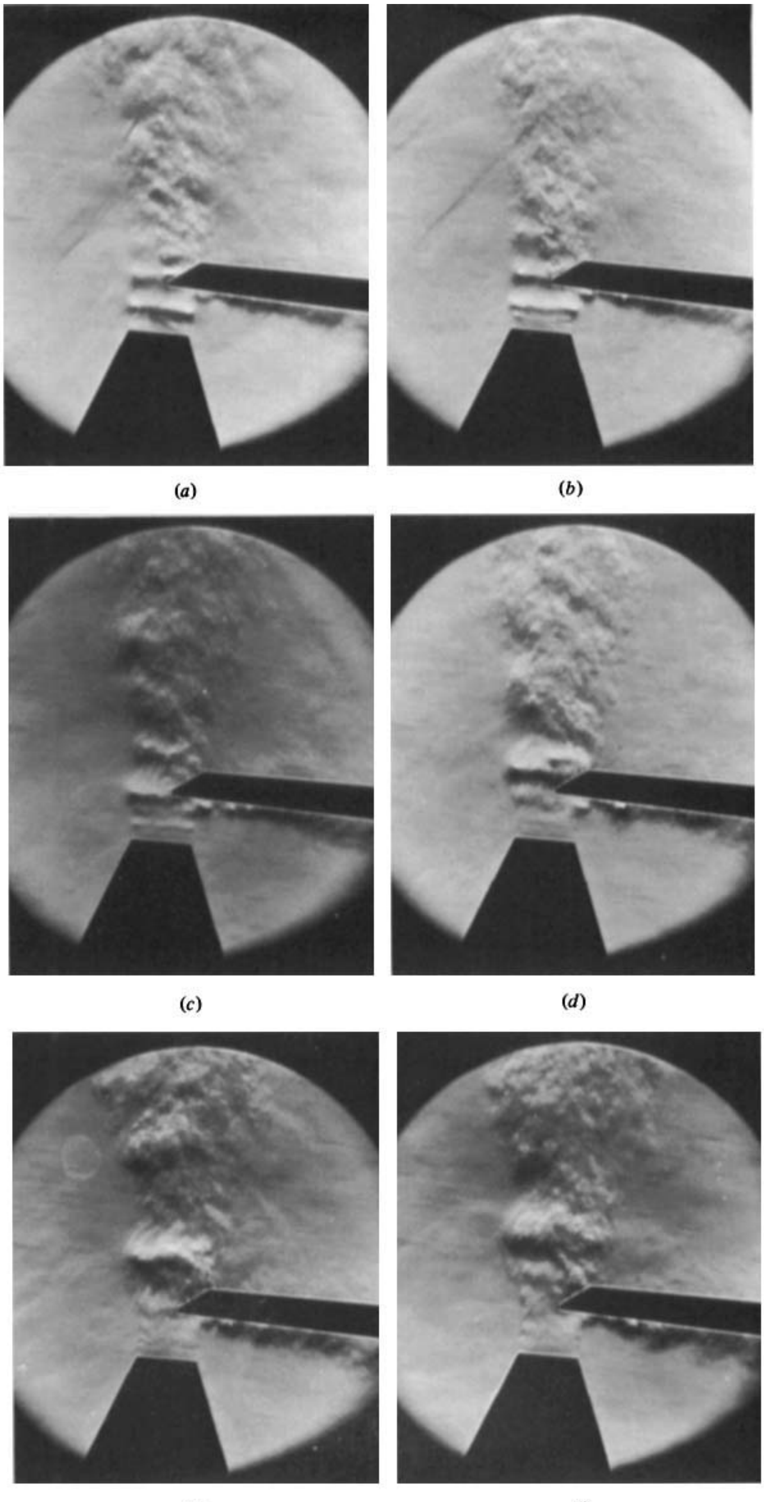

(a) (b) (c) (d) (e) (f)

FIGURE 4. Schlieren photographs of the excited jet (with sharp edge). Location of sharp edge: $x/D = 0{\cdot}75$, $y/D = 0{\cdot}15$. Other details as for figure 1.

using linear regression, usually having a correlation coefficient higher than 0·99. For the case of $x/D = 0{\cdot}3$, $y/D = 0{\cdot}15$ the convection velocity of the weak vortex is only $0{\cdot}4\,\overline{U}_0$, compared with $0{\cdot}5\,\overline{U}_0$ to $0{\cdot}6\,\overline{U}_0$ for those further downstream. For other locations of the sharp edge its velocity varies from $0{\cdot}5\,\overline{U}_0$ to $0{\cdot}6\,\overline{U}_0$ and is very marginally lower than that of the jet without the sharp edge, about $0{\cdot}6\,\overline{U}_0$. The convection velocities of the first and second N-vorticies are also shown in table 2. Generally, those of the first N-vortex are very marginally smaller than, while those of the second N-vortex are the same as, those of the uninterrupted vortices. In addition, the convection velocities of these two vortices are independent of the position of the sharp edge.

As has been discussed by Batchelor (1967, p. 524), the speed of travel of the vortex ring depends approximately on the ratio of its total kinetic energy to its fluid impulse. In the present investigation, the fluid impulse for the formation of the vortex ring is the same as that without the sharp edge. The presence of the sharp edge, however, would reduce the total kinetic energy of the vortex ring, though very slightly. This may be the reason for the very slight reduction in the convection velocity shown in table 2. From the slightly lower convection velocity observed in the cases very near the nozzle exit it seems that the presence of the sharp edge at these positions has a slightly greater effect on the total kinetic energy. The reason for this slightly higher reduction in convection velocity is not known but it may be due partly to the interruption in flow at this early developing stage.

4.2. *Wake behind the sharp edge*

Since the sharp edge is placed normal to the jet, it is to be expected that a wake will be formed behind it. The present situation, however, is different from the investigation of the wake flow behind a flat plate of other workers in that the flow distribution upstream of the sharp edge is not uniform. The mean velocity distribution depends on the location of the sharp edge (Townsend 1956; Davies, Fisher & Barratt 1963). In other words, besides other factors such as the configuration of the sharp edge itself and the Reynolds number of the jet, the wake formed behind the sharp edge would depend on its position and the distribution of flow over it.

Throughout the present study the vertex of the sharp edge is always located inside the potential core. For the cases of $x/D \leqslant 2$, $y/D \leqslant 0{\cdot}5$ a certain amount of its surface area is within the potential core and has a flow of constant mean velocity $\overline{U}_0$ over it. For the case of $x/D = 3$, $y/D = 0{\cdot}15$ and other cases of $y/D = 0{\cdot}35$ the vertex of the sharp edge is located just within the potential core. This means that only a very small portion of the surface is exposed to the flow of constant mean exit velocity $\overline{U}_0$. The remaining part of the sharp edge is under the influence of flow having non-uniform velocity distribution.

Schlieren photographs obtained with the sharp edge located very near the nozzle exit, at $x/D = 0{\cdot}3$, $y/D = 0{\cdot}15$, indicate that, owing to the absence of the jet vortices behind the sharp edge, the wake can be distinguished (figure 2*a*). The wake seems to extend into the main jet flow, at an angle to the jet axis. The effect that it has on the jet vortices can be seen from the changes of the coherent part of the second N-vortex which extend into the wake. As shown in figure 2(*b*, *c*), the extra mixing of the turbulence of the wake with the coherent part of the vortex, which extends into the wake, results in the more rapid diffusion of the coherent structure and its more rapid disappearance (figure 2*d*).

The outer boundary of the wake with the ambient air does not have the wavy structure of that with the main jet flow. This outer boundary has a more or less constant spread or angle, which tends to be slightly bigger than that of the main jet flow (figure 2*b*). However, during the passage of the strong second *N*-vortex the outer boundary is also disturbed. Nevertheless, this disturbance which extends into the surrounding ambient air is mainly found further downstream when the wake loses its intensity (figure 2*f*).

When the sharp edge is located further towards the outer boundary of the jet with the ambient air ($y/D = 0{\cdot}35$), the effect of its wake is less (figure 3). The angle of spread of the wake, as shown in figure 3 (*a*, *b*), seems to be less than that when the sharp edge is located nearer the jet axis. In addition, the intensity of this wake is lower, resulting in the dominance of the main jet flow and its vortices (figure 3*d*, *f*). However, it is interesting to find that during the passage of the strong second *N*-vortex, part of the fluid of the wake is being forced out into the ambient air and is distinctly shown in figure 3 (*d*). This part of the fluid becomes more diffuse as the second *N*-vortex convects further downstream (figure 3*e*, *f*). This observation means that at this radial position, because of the small interrupted area and the smaller wake of the sharp edge, the strong second *N*-vortex overcomes this interruption. The effect of the wake on the coherent ring structure of this jet vortex is much less. Nevertheless, a certain amount of loss of intensity, though small, is found at the region directly behind the sharp edge (figure 3*c*–*e*). Furthermore, the fluid of the wake does not intermix much with the coherent part of the strong vortex which extends into the wake. This results in the wake being forced into the ambient air (figure 3*d*, *f*).

Bauer (1961), Tam (1974) and Davis (1975) found vortices shedding from thin flat plates and aerofoils parallel to the free stream. In the present case the vortices shed by the sharp edge are shown in some of the schlieren photographs taken (figure 4*a* and figure 5*a*–*d*). They grow as they propagate downstream (figure 5*c*). Coupled with the growth is the more diffuse state of the vortex. The same effect is clearly shown at the location $x/D = 1{\cdot}0$, $y/D = 0{\cdot}15$ where the wake vortices shed by the vertex are found excited by the turbulence or disturbances associated with the main jet flow (figure 5*a*–*c*). These excited wake vortices are intense, especially the one at the axial position of $x/D = 2{\cdot}2$.

Besides being excited by the disturbances associated with the jet, the wake vortices are also found to be excited by both the weak-vortex and the first *N*-vortex (figure 5*b*–*d*). No wake vortex is found during and after the passage of the strong second *N*-vortex. This absence may be due to the high intensity of this strong second *N*-vortex so that the wake vortices are masked. In other words, the intensity of this strong vortex is higher than the saturated level of the wake vortex, resulting in its masking (Crow & Champagne 1971; Moore 1977). The other reason may be due to the Strouhal number of the excitation being different from the most preferred mode of the wake vortex (Crow & Champagne 1971; Kwan & Ko 1977).

The wake vortices are also observed when the sharp edge is at $x/D > 1{\cdot}0$, $y/D = 0{\cdot}15$. They are similar to those illustrated in figure 5 and thus are not shown in this presentation.

The approximate angle of propagation of the wake vortices is correlated with the normalized inner area of the part of the sharp edge which is located inside the potential core (figure 6). In other words, the inner area is the area within the uniform flow of $\overline{U}_0$.

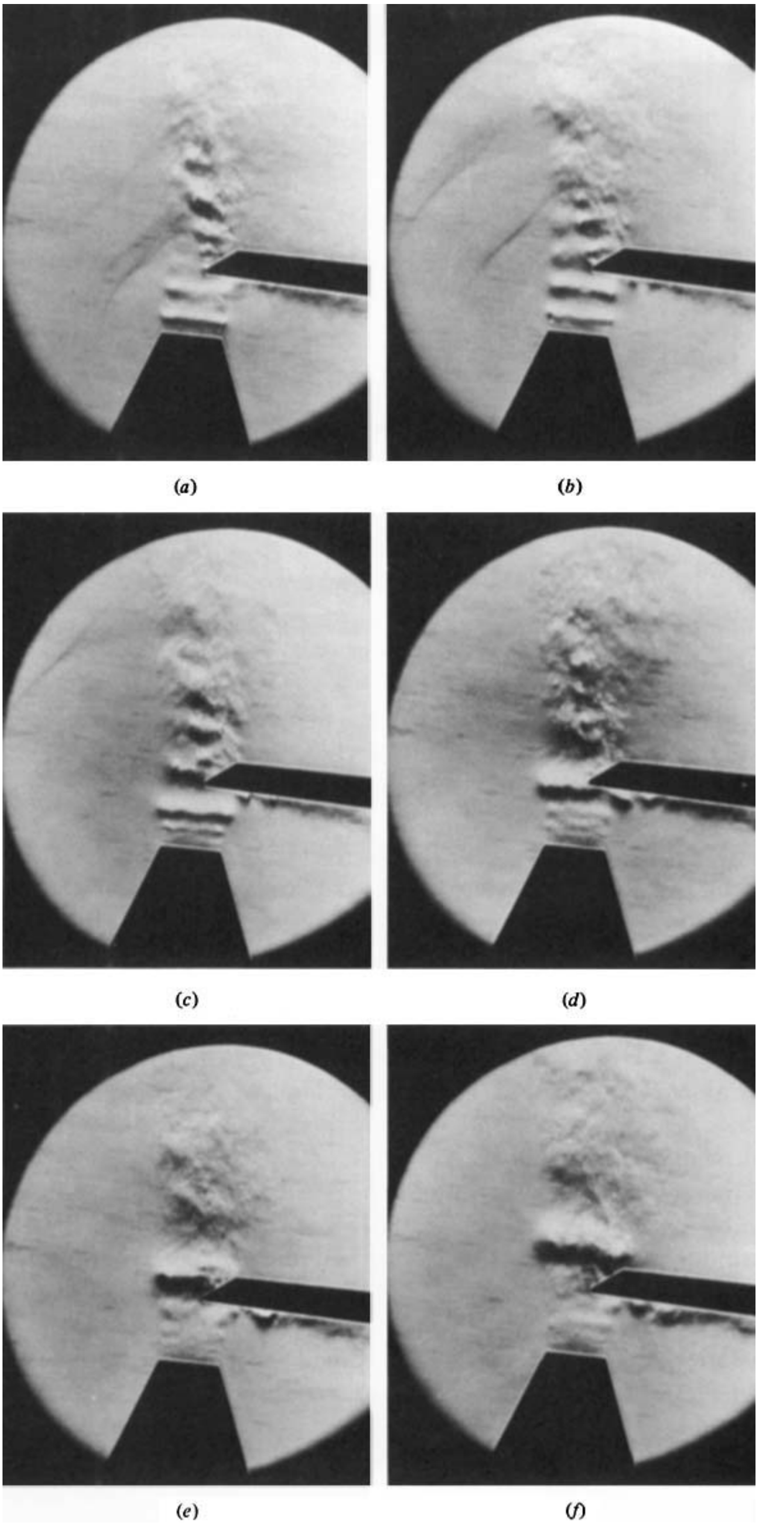

(a) (b) (c) (d) (e) (f)

FIGURE 5. Schlieren photographs of the excited jet (with sharp edge). Location of sharp edge: $x/D = 1{\cdot}0$, $y/D = 0{\cdot}15$. Other details as for figure 1.

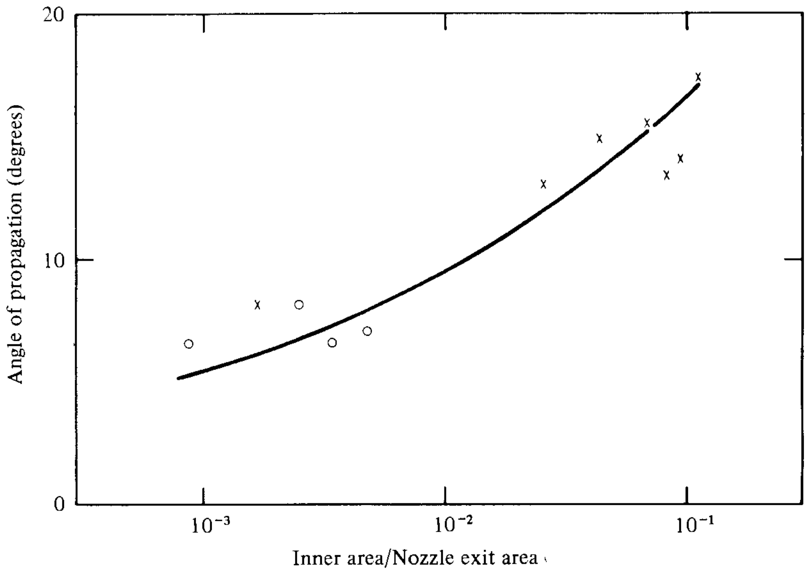

FIGURE 6. Variation of approximate angle of propagation with inner area. y/D: ×, 0·15; ○, 0·35. ——, Batchelor.

The figure seems to suggest that the bigger the inner area within the potential core the bigger the angle of propagation. It attains a value of about 16° when the inner area is 10 % of the nozzle exit area. It reduces to a minimum angle of about 8° when the inner area ratio is less than one per cent.

The data also indicate that whenever the vertex of the sharp edge is located just within the inner boundary of the jet (that is, the boundary between the mixing region and the potential core), the angle is about 8°. Likewise, the angle of this inner boundary with the jet axis is about 6° (Ko & Davis, 1971). At this stage it is not known how significant the agreement of these two angles is. It may suggest that the potential core is the more favoured path of the wake vortices. This suggestion may be reasonable, The findings of Ko & Davis (1975) and Kwan & Ko (1977) were that jet vortices convect downstream along the constant $\eta(y-\frac{1}{2}D)/x$ line, at which the mean velocity is constant. Thus, it may not be surprising that the wake vortices also propagate within the constant mean velocity region.

From the theoretical consideration of two-dimensional flow past a flat plate with a cavity at ambient pressure (Batchelor 1967, p. 497) the cavity may be expected to extend to infinity downstream. The cavity boundary is asymptotic to the parabola $y^2 = 8bx/(\pi+4)$, where $2b$ is the breadth of the plate. Based on the assumption that b is the distance of the sharp edge which is inside the potential core, the angles at an arbitrary distance of one diameter downstream of the sharp edge were estimated and are shown in figure 6. It is interesting that good agreement is found between the approximate angle of propagation and the calculated angle of the cavity boundary at one diameter downstream. However, this comparison is only true if a further assumption is valid, viz. that the path of propagation of the visualized wake vortices is either at or parallel to the boundary behind the sharp edge.

The convection velocities $(\overline{U}_c)_w$ of the wake vortices could similarly be estimated

Location of sharp edge		Convection velocity $(\overline{U}_c)_w/\overline{U}_0$	
x/D	y/D	Weak vortex	First N-vortex
0·55	0·15	0·4	0·4
0·75	0·15	0·5	0·5
1·0	0·15	0·5	0·4
1·5	0·15	0·4	0·5
2·0	0·15	0·4	—

TABLE 3. Convection velocity of the wake vortices.

from the sequence of schlieren photographs obtained with different time delay (table 3). From the table the convection velocity of the weak and first N-vortex can be seen to be roughly the same, about $0{\cdot}4\,\overline{U}_0$ to $0{\cdot}5\,\overline{U}_0$, that is independent of the location of the sharp edge. When compared with the convection velocities of similar vortices in the main jet flow (table 2), it is found that the wake vortices convect at a slightly lower velocity. Based on the above convection velocities and the wavelength, an estimated frequency of 14–20 kHz with an average of about 17 kHz is found.

4.3. *Flow on the surface of the sharp edge*

Owing to the obstruction of the sharp edge, the flow upstream from the edge is redirected and flows along the surface of the sharp edge. This redirection implies that this flow inherits, at least to a certain extent, the properties of the jet. Further, the redirection also implies that not only is the flow in the potential core redirected but also the flow in the mixing region. Thus, there is a certain amount of mixing and interaction of these flows of different velocities. In addition, any disturbances, which are present in the jet flow, are also redirected and convect along the surface of the sharp edge. This flow is not really a boundary layer as such. Rather, it is a redirected free shear flow which is under the additional influence of the friction of the surface of the edge. Even though the free shear flow of the jet has been redirected by 90°, it is to be expected that shearing with the ambient air would still occur (figures 2 and 4).

The wavy patterns on the boundary may be due to the redirected jet vortices of the main jet flow. This means that any unstable disturbances formed near and just outside the nozzle exit continue to grow even after their redirection. This redirection of the disturbances can be seen from the excited vortices being redirected by the sharp edge at $x/D = 0{\cdot}3$, $y/D = 0{\cdot}15$ (figure 2*a*, *b*). In the former figure the redirected parts of the weak, first and second N-vortex are clearly shown. However, these fairly coherent parts of the vortices experience very rapid diffusion and disintegrate at a distance of about half a jet diameter (figure 2*c*, *e*). The disintegration of the redirected vortex on the sharp edge surface is illustrated from the second N-vortex which undergoes a sudden increase in size which amounts to a doubling of the original size. Although the coherent part disintegrates, it still convects further along the surface before it is completely diffused (figure 2*f*).

This sudden increase in size or the disintegration of the coherent part is absent in the main jet flow. This may be due to the continuous development of the vortex and the additional effect of the surface which does not allow free growth in that direction. In this respect, the effect on the boundary with the ambient air accumulates and

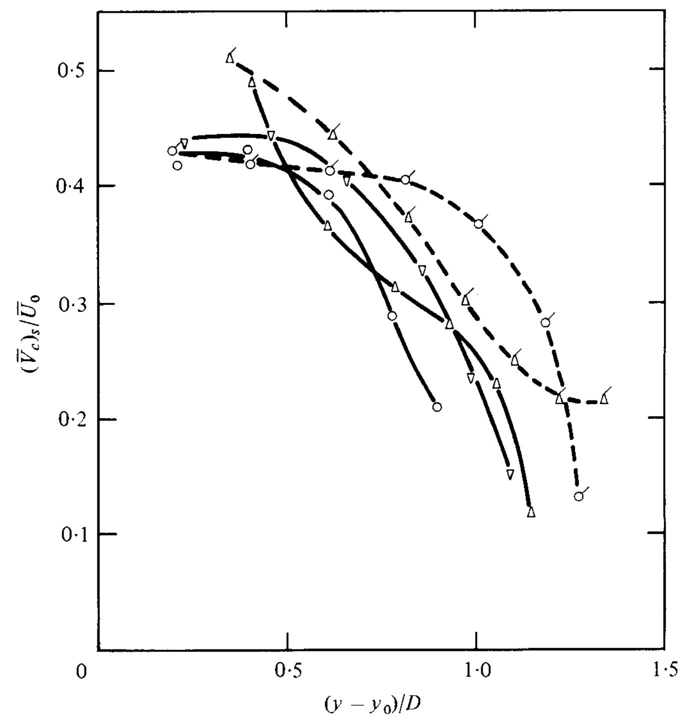

FIGURE 7. Convection velocity of weak and first N-vortex along the surface of the sharp edge (y/D = 0·15). Weak vortex, x/D: ó, 0·75; △́, 1·0. First N-vortex, x/D: ○, 0·75; △, 1; ▽, 1·5.

reaches such an unstable state that instantaneous disintegration or separation of the coherent part from the surface occurs.

When the sharp edge is located further downstream, the vortices of the main jet flow are more developed before their arrival and redirection along the surface. Thus, the schlieren photographs obtained at x/D = 1·0, y/D = 0·15, show the convection of the more coherent parts of the weak, first and second N-vortex along the surface (figure 5c, e). The coherent part of these vortices seems to disintegrate further along the surface than for those at x/D = 0·3. The growth in size accompanied by the disintegration of the coherent part of the second N-vortex is not as dramatic (figure 5f) as that when the sharp edge is located further upstream (figure 2c). This may be due to the more complete growth of this jet vortex before its arrival at the sharp edge and thus the lesser growth after redirection. The accumulative effect is correspondingly less.

When the sharp edge is located further away from the jet axis, only a very small portion of the vortices is interrupted and redirected along the surface of the sharp edge. For the case of x/D = 0·3, y/D = 0·35 the disintegration of the coherent part of the second N-vortex occurs fairly soon after its redirection (figure 3b, c). The same reason of the continuous growth of the redirected part of the vortex and the accumulated effect of the surface on its disintegration may be applied.

The convection velocities $(\overline{V}_c)_s$ along the surface of the sharp edge were estimated. The adopted time delay interval of 38 μs between successive schlieren photographs

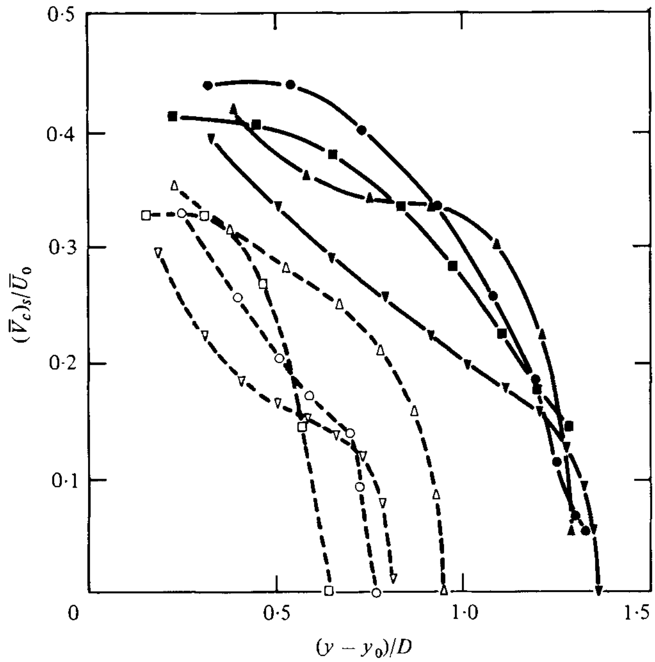

FIGURE 8. Convection velocity of second N-vortex along the surface of the sharp edge. y/D = 0·15: ▼, 0·3; ■, 0·55; ●, 0·75; ▲, 1·0. y/D = 0·35: ▽, 0·3; □, 0·55; ○, 0·75; △, 1·0.

allowed the progress of each vortex to be followed. However, linear relationship of the x–t diagram was not obtained and a fourth-order polynomial was fitted to the data.

The convection velocities thus estimated for the weak vortex and first N-vortex and for the second N-vortex are shown in figure 7 and 8 respectively. The non-dimensional radial distance is based on y_0 which is the radial position from the jet axis at which the vortex arrives at the sharp edge. The general trend of the convection velocity is its decrease as the individual vortex convects further along the surface. This decrease in the convection velocity suggests its continuous deceleration before its loss of identity or when the diffusion is at such a state that it is extremely difficult to estimate its position. For the case of the second N-vortex the convection velocity is generally higher when the sharp edge is located nearer to the jet axis at $y/D = 0{\cdot}15$ (figure 8). The distance before its disappearance is also bigger. This may be due to the bigger portion of the vortex being redirected by the sharp edge, that is, a bigger amount of energy is available to maintain its propagation along the surface.

The convection velocities $(\bar{V}_c)_s$ immediately after their redirection and the ratio $(\bar{V}_c)_s/(\bar{U}_c)_j$ with those before redirection are tabulated in table 4. The loss of energy during the redirection of the weak vortex and first N-vortex results in the lower convection velocity being found. The amount of reduction is about 20 % of their original convection velocity. For the stronger second N-vortex, however, no loss is found for the case at $y/D = 0{\cdot}15$. For the cases at $y/D = 0{\cdot}35$, however, a similar loss to that of the weak and first N-vortex is found.

The loss in the kinetic energy or the convection velocities incurred during the re-direction is to be expected. It is not, however, expected that no indication of the loss is

Location of sharp edge		$(\bar{V}_c)_s/\bar{U}_0$ $[(\bar{V}_c)_s/(\bar{U}_c)_i]$		
x/D	y/D	Weak vortex	First N-vortex	Second N-vortex
0·3	0·15	—	—	0·4 [1·0]
0·55	0·15	—	0·5 [1·0]	0·4 [1·0]
0·75	0·15	0·4 [0·8]	0·4 [0·8]	0·4 [1·0]
1·0	0·15	0·5 [1·0]	0·5 [1·0]	0·4 [1·0]
1·5	0·15	—	0·4 [0·7]	0·4 [1·0]
2·0	0·15	—	0·5 [1·0]	—
0·3	0·35	—	—	0·3 [0·8]
0·55	0·35	—	—	0·3 [0·8]
0·75	0·35	—	—	0·3 [0·8]
1·0	0·35	—	—	0·4 [1·0]
1·5	0·35	—	—	0·4 [1·0]

TABLE 4. Convection velocity of the vortices immediately after their redirection along the surface of the sharp edge.

incurred for the strong second N-vortex which is redirected by the sharp edge located at $y/D = 0{\cdot}15$ while loss is found when the sharp edge is located further outside ($y/D = 0{\cdot}35$). The reason for this absence of any loss during the redirection of the vortex is not really known. It may be due to the high inherited energy of the vortex itself.

5. Conclusions

The extensive schlieren photographs of an excited jet, which is interrupted by a 90° sharp edge, isolate three distinct flows: the main jet flow itself, the wake behind the sharp edge and the flow on the surface of the sharp edge. Within the range of the sharp edge considered in the present investigation all three flows are found.

The acoustic disturbance is introduced upstream of the nozzle exit. The introduced excitation results in the formation of the weak vortex, the first and second N-vortex within the jet flow. It is mainly through the observation of the progress of these vortices and the interruption by the sharp edge that the change of flow characteristics and pattern can be found.

The amount of change of the flow characteristics of the main jet flow and its three vortices depends on the location of the sharp edge, both axially and radially. Although the vortices seem not to be affected before their arrival at the sharp edge, they are found to be modified after this interruption. Since the part of the vortex, which is interrupted and redirected along the surface of the sharp edge, is lost, readjustment of the rest of the vortex occurs further downstream. The ability and speed of readjustment depends on the initial strength of the vortex before the interruption. The stronger one tends to be more able to adjust than the weaker one. The readjustment, which involves loss of energy, results in the quicker diffusion and earlier disappearance of the vortex. This also results in the lower estimated convection velocity. The reduction in the convection velocity is slightly greater for the weaker vortices than for the strong second N-vortex.

The effect of the sharp edge on the vortices in the main jet flow seems to be greater when it interrupts the vortices at their developing stage. The vortex is found to require an axial distance of one to one and a half diameters from the nozzle exit to develop to its strongest condition. Thus, the closer the sharp edge to the nozzle exit, the greater the influence on the less-developed vortex. This is the reason why the convection velocity and the distance of the disappearance of the vortex are found to be lower at these locations.

The wake flow formed behind the sharp edge seems to interact with the main jet flow. This interaction produces occasional change in the flow characteristics on both the main jet flow and on the wake. The amount of change also seems to depend on the location of the sharp edge and also on the strength of the jet vortices.

This wake is also excited by the disturbances due to the passage of the weak and first N-vortex. This excitation of the wake vortices allows both the convection velocity and the wavelength to be estimated. The convection velocity estimated is found to be fairly constant and is slightly lower than that of the jet vortices. The derived frequency of the wave vortices is in the high frequency regime, about 17 kHz.

The propagation of the wake vortices downstream seems to make an angle θ with the jet axis. This angle seems also to depend on the inner area of the sharp edge inside the potential core. It seems from the present investigation that the uniform flow inside the potential core is the dominant factor on the angle. The flow of varying mean velocity of the mixing region seems not to affect the direction of propagation of the wake vortices much.

Although the wake vortices have been excited by the disturbances associated with the weak and first N-vortex, no indication of wake vortices has been observed during the passage of the stronger second N-vortex. This may be due to the masking of the weak wake vortices by the disturbances associated with the stronger second N-vortex.

The flow on the surface of the sharp edge is due to the redirection of the main jet flow. Besides the presence of free shear, the friction of the surface is another factor which affects the flow. Further, any disturbances or vortices present in the main jet flow are interrupted by the sharp edge and redirected along the surface. Owing to the loss of energy during their redirection, the vortex of lower kinetic energy seems to be more susceptible to the combined effect of free shear and of the friction of the surface. This results in the sudden disintegration of the coherent part of the vortex and its earlier disappearance.

The work was carried out while the author was awarded a Commonwealth Academic Staff Fellowship tenable in the Engineering Department, University of Cambridge. The author wishes to thank The Association of Commonwealth Universities for the kind award.

The author further wishes to express his thanks to the Science Research Council for the facility and technical assistance provided through the good offices of a SRC grant to Prof. J. E. Ffowcs Williams.

The author also wishes to thank Prof. J. E. Ffowcs Williams and Dr S. N. Heavens for their kind guidance and valuable suggestions. The technical assistance of Mr N. Eshelby was important for the completion of the study. The author further wishes to thank Miss K. E. Barker for her comment and advice during the preparation of the manuscript. Lastly, the author wishes to thank his wife who did most of the photographic work.

REFERENCES

ARCTANDER, C. L., HODGE, C. G. & TATE, R. B. 1975 Development of noise-reduction concepts for 727 and 737 airplanes. *J. Acoust. Soc. Am.* **58**, 155–172.

ARNDT, R. E. A., FUCHS, H. V. & MICHEL, U. 1978 Laboratory study of jet-noise suppressors. *J. Acoust. Soc. Am.* **63**, 1060–1068.

ARNDT, R. E. A., TRAN, N. C. & BAREFOOT, G. 1974 Turbulence and acoustic characteristics of screen perturbed jets. *A.I.A.A. J.* **12**, 261–262.

BATCHELOR, G. K. 1967 *An Introduction to Fluid Dynamics.* Cambridge University Press.

BAUER, A. B. 1961 Vortex shedding from thin flat plates parallel to the free stream. *J. Aerospace Sci.* **28**, 340–341.

CHAN, Y. Y. 1974 Spatial waves in turbulent jets. *Phys. Fluids* **17**, 46–53.

CROW, S. C. & CHAMPAGNE, F. H. 1971 Orderly structure in jet turbulence. *J. Fluid Mech.* **48**, 547–591.

DAVIES, P. O. A. L., FISHER, M. J. & BARRATT, M. J. 1963 The characteristics of turbulence in the mixing region of a round jet. *J. Fluid Mech.* **15**, 337–367.

DAVIS, S. S. 1975 Theory of discrete vortex noise. *A.I.A.A. J.* **13**, 375–380.

DONALDSON, C. D. & SNEDEKER, R. S. 1971 A study of free jet impingement. Part 1. Mean properties of free and impinging jets. *J. Fluid Mech.* **45**, 281–319.

DONALDSON, C. D., SNEDEKER, R. S. & MARGOLIS, D. P. 1971 A study of free jet impingement. Part 2. Free jet turbulent structure and impingement heat transfer. *J. Fluid Mech.* **45**, 477–512.

FRASCA, R. L. 1975 Noise-reduction programs for DC-8 and DC-9 airplanes. *J. Acoust. Soc. Am.* **58**, 173–191.

FUCHS, H. V. & MICHEL, U. 1977 Experimental evidence of turbulence source coherence effecting jet noise. *A.I.A.A. Paper* no. 77–1348.

HEAVENS, S. N. 1978 Visualization of unsteady jets and aerodynamic noise fields. *13th Int. Cong. on High Speed Photography and Photonics*, paper TS14-2, 86. Tokyo.

HEAVENS, S. N. 1980 Visualization of the acoustic excitation of a subsonic jet. *J. Fluid Mech.* **100**, 185–192.

KO, N. W. M. & DAVIES, P. O. A. L. 1971 The near field within the potential cone of subsonic cold jets. *J. Fluid Mech.* **50**, 49–78.

KO, N. W. M. & DAVIES, P. O. A. L. 1975 Some covariance measurements in a subsonic jet. *J. Sound Vib.* **41**, 347–358.

KWAN, A. S. H. & KO, N. W. M. 1977 Covariance measurements in subsonic coaxial jets. *J. Sound Vib.* **52**, 567–578.

LAU, J. C., FISHER, M. J. & FUCHS, H. V. 1972 The instrinsic structure of turbulent jets. *J. Sound Vib.* **22**, 379–406.

MOORE, C. J. 1977 The role of shear-layer instability waves in jet exhaust noise. *J. Fluid Mech.* **80**, 321–367.

ROCKWELL, D. O. & NICCOLLS, W. O. 1972 Natural breakdown of planar jets. *Trans. A.S.M.E.* D, *J. Basic Engng* **94**, 720–730.

ROSHKO, A. 1976 Structure of turbulent shear flows: a new look. *A.I.A.A. J.* **14**, 1349–1357.

SCHARTON, T. D. & WHITE, P. H. 1972 Simple pressure source model of jet noise. *J. Acoust. Soc. Am.* **52**, 399–412.

SFORZA, P. M., STASI, W., PAZIENZA, J. & SMORTO, M. 1978 Flow measurements in leading-edge vortices. *A.I.A.A. J.* **16**, 218–224.

TAM, C. K. W. 1974 Discrete tones of isolated airfoils. *J. Acoust. Soc. Am.* **55**, 1173–1177.

TOWNSEND, A. A. 1956 *The Structure of Turbulent Shear Flow.* Cambridge University Press.